Check for updates

RESEARCH ARTICLE doi.org/10.1002/adsc.202500354

ADVANCED SYNTHESIS & CATALYSIS

Synergistic Visible Light Nanophotocatalysis and Asymmetric Organocatalysis for the Stereoselective α-Alkylation of Aldehydes

Antonio Di Sabato,[a] Marta Santoni,[a] Vyali Georgian Moldoveanu,[a] Alessandro Camilli,[a] Marta Feroci,[b] Giorgio Olivo,[a] Beatrice Simonis,[c] Elisa Sturabotti,[d] Francesca Leonelli,[a,*] and Fabrizio Vetica[a,*]

[a] Department of Chemistry, Sapienza University of Rome, Piazzale Aldo Moro 5, 00185 Rome, Italy
E-mail: francesca.leonelli@uniroma1.it; fabrizio.vetica@uniroma1.it
[b] Department of Basic and Applied Sciences for Engineering (SBAI), Sapienza University of Rome, via Castro Laurenziano, 7, 00161 Rome, Italy
[c] CNR-Institute for Biological Systems (CNR-ISB) - Secondary Office of Rome, Reaction Mechanisms c/o Chemistry Department, Sapienza University, Piazzale Aldo Moro 5, 00185 Rome, Italy
[d] Center for Cooperative Research in Biomaterials (CIC biomaGUNE), Basque Research and Technology Alliance (BRTA), Paseo de Miramón 194, 20014 Donostia-San Sebastián, Spain

Manuscript received: March 28, 2025; Revised manuscript received: April 28, 2025;
Version of record online:

Supporting information for this article is available on the WWW under https://doi.org/10.1002/adsc.202500354

Abstract: Carbon dots (CDs) are privileged carbon-based nanomaterials which they have been extensively studied in recent years in catalysis. In fact, their peculiar photoluminescence features have found applications in nanophotocatalysis as well as bioimaging and sensing. Nevertheless, their application as nanophotoredox catalysts in stereoselective transformations is still unexplored. Herein, this study reports the combination of carbon dots as nanophotocatalysts and asymmetric organocatalysis for the stereoselective α-functionalization of aldehydes. Employing various bromo-derivatives as alkylating agents, it achieves the corresponding enantioenriched α-alkylated derivatives with excellent yields (up to 94%) and enantioselectivities (up to 98:2 e.r.). With a series of control experiments, cyclic voltammetry and fluorescence quenching studies, it is possible to postulate a synergistic dual catalytic cycle that involves a photo-oxidative quenching of the excited stated of CDs paired with an enamine activation promoted by the MacMillan organocatalyst followed by radical alkylation. This study successfully demonstrates that carbon dots can efficiently replace metal-based photocatalysts, promoting photoredox catalytic stereoselective transformations even at low concentrations (down to 0.1 mg mL^{-1}), paving the way to more sustainable and possibly recyclable catalytic systems.

Keywords: asymmetric organocatalysis, carbon dots, nanophotocatalysis, photoredox catalysis, synergistic catalysis

1. Introduction

Carbon dots (CDs) are an emerging class of low-cost and biocompatible nanomaterials which has addressed the attention of the scientific community in recent years. Due to their peculiar photoluminescence and structural features, such as quasi-spherical dimensions below 10 nm and a tunable and easy-modifiable active surface, they represent a multi-applicative nanomaterial platform for catalysis, photocatalysis, sensing, and nanomedicine.[1] For instance, the photoluminescent and optical properties of CDs, which are easily tunable by modification of synthetic procedure and heteroatom doping, have been employed for photo-activated transformations, such as photodegradation of pollutants but also for organic synthesis.[2] Moreover, their biocompatibility, easy surface modifications, and excellent suspensibility in both aqueous and organic solvents make CDs excellent candidates as heterogeneous and recyclable catalysts. The combination of photocatalysis and stereoselective organocatalysis represents an innovative and rapidly growing field of research, paving the way to new horizons in stereoselective synthetic methodologies for the preparation of enantioenriched compounds.[3] In 2008, MacMillan et al. reported a seminal work for the stereoselective α-functionalization of aldehydes

 © 2025 Wiley-VCH GmbH

combining a photoreducing reactivity of a ruthenium-based photocatalyst and a chiral imidazolidinone organocatalyst (**Figure 1**a).[4] This work unlocked the asymmetric α-alkylation of aldehydes with alkyl bromides bearing electron-withdrawing groups, which are typically poorly reactive in classical 2-electron alkylation protocols. Afterward, the combination of photoredox catalysts and asymmetric organocatalysis has experienced an exponential growth.[5]

The environmental concerns of last decade are driving a growing demand to replace current photosensitizers, typically based on expensive and toxic Ru and Ir complexes, with more sustainable and easy-to-prepare ones. In fact, the possibility to replace metal-based photosensitizers with organic molecules[6] or by employing the intrinsic optical properties of reaction intermediates (e.g., electron donor–acceptor (EDA) complexes)[7] is being currently investigated.

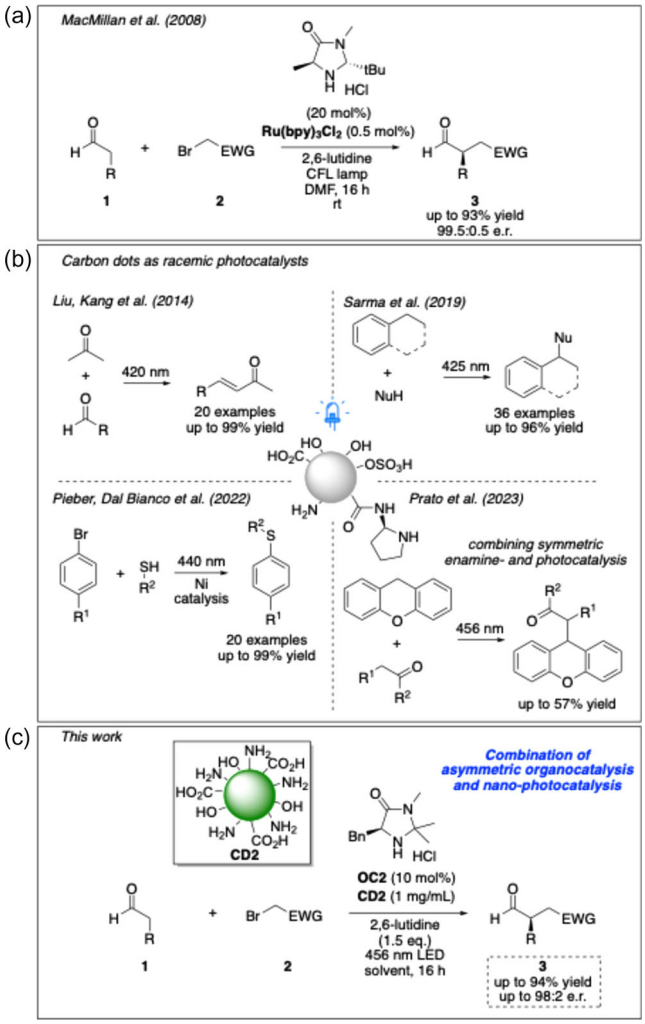

Figure 1. Synergistic photoredox catalysis and asymmetric organocatalysis in organic synthesis: a,b) state of the art and c) this work.

For instance, Alemán and coworkers reported the synthesis of a novel imidazolidinone-based organocatalyst to perform the MacMillan reaction, with the chromophoric photosensitizer embedded in the chiral catalyst, thus avoiding the use of ruthenium complexes.[6b]

Within this context, in recent years CDs have been efficiently applied as sustainable and easy-to-prepare nanophotocatalysts to promote organic transformations such as aldol reaction,[8] C–C couplings,[9] cross-coupling reactions,[10] cycloaddition reactions,[11] and perfluoroalkylations (Figure 1b).[12] In these reports, the photocatalytic activity of CDs is strictly connected to their photoluminescence properties upon absorption of visible light. For instance, Liu and Xing studied the effect of nitrogen doping on the photocatalytic performances of CDs in cross-coupling reactions in water,[10d] evidencing how an increased N-doping decreases catalytic efficiency.

However, the application of CDs as photoredox catalysts for stereoselective synthetic methodologies is still unprecedented. Due to our recent interest in CDs chemistry for stereoselective catalytic transformations,[13] biomedical applications[14] and photochemistry,[15] we envisioned a possible application of CDs with the MacMillan organocatalyst for the asymmetric α-alkylation of aldehydes.

2. Results and Discussion

Our investigation started by the synthesis of photoactive CDs, which was accomplished based on our previously reported work.[14] Specifically, we selected two classes of CDs, possessing similar dimensions (≈2–3 nm), but different surface functional groups and polarization (determined by X-ray photoelecton spectroscopy (XPS), dynamic light scattering (DLS), zeta potential, and atomic force microscopy (AFM)) (**Scheme 1**). We identified these nanomaterials as potential model photocatalyst due to their fluorescence emission upon excitation with blue light ($\lambda^{exc}_{max} = 440$ nm for **CD1** and 420 nm for **CD2**). Moreover, being **CD1** derived by a chiral compound, their active surface is chiral, and thus, a possible combination of their chirality with their photoredox properties could be of potential interest for the envisioned stereoselective alkylation reaction.

With the designed nanophotocatalysts in hand, we selected hydrocinnamaldehyde (**1a**) and bromomalonate (**2a**) as model substrates to perform the MacMillan α-functionalization, using a Kessil lamp emitting blue light at 456 nm (**Table 1**). Initially, we decided to employ the Jørgensen–Hayashi catalyst **OC1** as asymmetric organocatalyst. As previously mentioned, since the CDs **CD1** are chiral, we decided to test the model reaction in the sole presence of these nanodots.

We observed the formation of a moderate amount of product, with low enantiomeric ratios (Table 1, entry 1).

© 2025 Wiley-VCH GmbH

16154169, 0, Downloaded from https://advanced.onlinelibrary.wiley.com/doi/10.1002/adsc.202500354 by Fabrizio Vetica - University Di Roma La Sapienza , Wiley Online Library on [16/06/2025]. See the Terms and Conditions (https://onlinelibrary.wiley.com/terms-and-conditions) on Wiley Online Library for rules of use; OA articles are governed by the applicable Creative Commons License

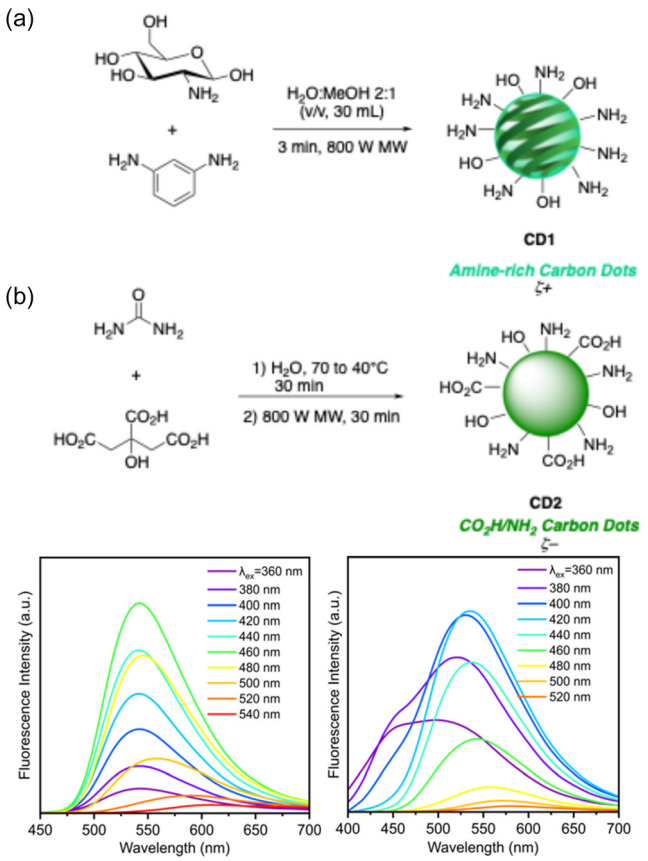

Scheme 1. Bottom-up synthesis of photoactive CDs; photoluminescent analysis of characterization of (left) **CD1** and (right) **CD2**.

Then, the presence of either 2,6-lutidine, **OC1**, or both was tested, highlighting that the reaction occurs in the absence of the photocatalyst with moderate yield and with 73.5:26.5 e.r. (Table 1, entry 2). The presence of 10 mg of **CD1** and 2,6-lutidine using the two different enantiomers of **OC1** afforded the desired product with comparable moderate yield and opposite enantiomeric ratio, indicating that the chirality of the nanodot **CD1** does not influence the stereoselectivity of the final product to a significant extent (Table 1, entries 3 and 4). We hypothesized that the low yield could be attributed to the intense dark color and turbidity of the reaction mixture due to the high amount of CDs, possibly impeding a complete light irradiation. In fact, by reducing the amount of **CD1**, the yield increased, with no negative influences on the e.r. value (Table 1, entries 5 and 6). Subsequently, we tested the activity of the MacMillan imidazolidinone catalyst, **OC2**. Pleasingly, we observed a substantial increase of both yield and enantioselectivity (55% yield, 94:6 e.r., Table 1, entry 7). The analogous experiment in the absence of either 2,6 lutidine or the photocatalyst highlighted a dramatic yield decrease, thus evidencing that the photocatalyst is influencing the reactivity (Table 1, entries 8 and 9). To our delight, by switching to photocatalyst **CD2**, employing both lutidine

Table 1. Catalysts screening for the synergistic nanophoto/organocatalytic alkylation of aldehyde 1a.

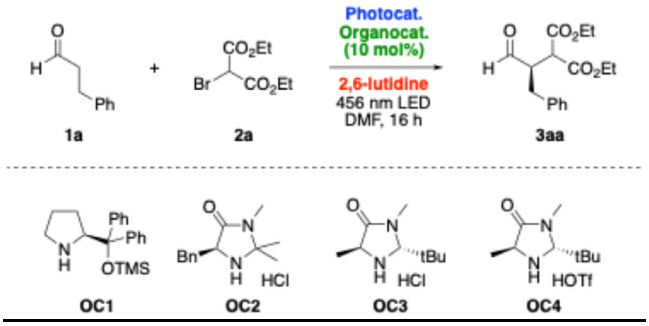

Entry[a]	Photocat. [mg mL^{-1}]	Organocat.	2,6-Lutidine [eq.]	Yield [%][b]	e.r.[c],[d]
1	**CD1** (10)	–	–	9	40:60
2	–	**OC1**	3	29	73.5:26.5
3	**CD1** (10)	**OC1**	3	13	72.5:27.5
4	**CD1** (10)	*ent*-**OC1**	3	16	28:72
5	**CD1** (1)	*ent*-**OC1**	–	11	30:70
6	**CD1** (1)	**OC1**	3	24	73.5:26.5
7	**CD1** (1)	**OC2**	3	55	94:6
8	**CD1** (1)	**OC2**	–	15	85:15
9	–	**OC2**	3	27	93:7
10	**CD2** (1)	**OC2**	3	72	95:5
11	**CD2** (1)	**OC2**	–	12	71:29
12	**CD2** (1)	**OC3**	3	74	91:9
13	**CD2** (1)	**OC4**	3	52	85:15

[a] Unless otherwise stated, the reaction conditions were: **1a** (0.2 mmol), **2a** (0.1 mmol), and *N*,*N*-dimethylformamide (DMF) (1 mL) at rt for 16 h under inert atmosphere and with degassed solvents;
[b] Yield determined via ^{1}H NMR analysis using the internal standard method;
[c] Determined via high performance liquid chromatography (HPLC) on a chiral stationary phase;
[d] First e.r. value corresponds to (*R*)-**3aa** as shown in the scheme.

and **OC2**, we could obtain the desired product in 72% yield and 95:5 e.r. (Table 1, entries 10–11). Interestingly, **OC3** and **OC4**, the optimal catalyst in MacMillan' seminal work, did not afford the title product with the same enantiomeric ratios (Table 1, entries 12–13), suggesting a synergistic chirality induction by CDs **CD2** and the organocatalyst in the enantioselective transition state.

Once identified the best combination of photo- and organocatalyst, we focused on the further optimization of the reaction conditions by testing the effects of different solvents, identifying *N*,*N*-dimethylformamide (DMF) as the optimum one for the alkylation reaction (see Table S3, Supporting Information). Subsequently, we decided to thoroughly study the influence of the CDs or 2,6-lutidine loading on the reaction conditions (**Table 2**). Hence, we systematically decreased the amount of **CD2** from 5 mg to 0.1 mg mL^{-1} at a 0.1 mmol scale (Table 2, entries 1–5). Interestingly, the yield

© 2025 Wiley-VCH GmbH

16154169, 0, Downloaded from https://advanced.onlinelibrary.wiley.com/doi/10.1002/adsc.202500354 by Fabrizio Vetica - University Di Roma La Sapienza , Wiley Online Library on [16/06/2025]. See the Terms and Conditions (https://onlinelibrary.wiley.com/terms-and-conditions) on Wiley Online Library for rules of use; OA articles are governed by the applicable Creative Commons License

Table 2. Reaction conditions optimization.

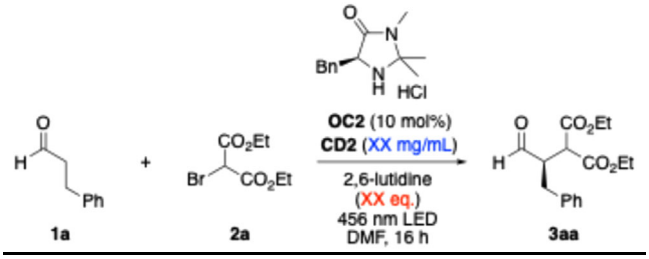

Entry[a]	CD2 [mg mL^{-1}]	2,6-lut. [eq.]	Y. [%][b]	e.r. [%][c],[d]
1	5	3	57	95:5
2	2	3	62	94.5:5.5
3	0.5	3	60	93.5:6.5
4	0.2	3	73	93.5:6.5
5	0.1	3	69	93.5:6.5
6	1	2	84	95:5
7	1	1.5	88	94.5:5.5
8	1	1.2	88	93.5:6.5
9	1	1	74	93:7
10	1	0.5	42	82:18

[a] Unless otherwise stated the reaction conditions were: **1a** (0.2 mmol), **2a** (0.1 mmol), and DMF (1 mL) at rt for 16 h under inert atmosphere and with degassed solvents;
[b] Yield determined via ^{1}H NMR analysis using the internal standard method;
[c] Determined via HPLC on a chiral stationary phase;
[d] Positive e.r. values corresponds to (*R*)-**3aa** as shown in the scheme.

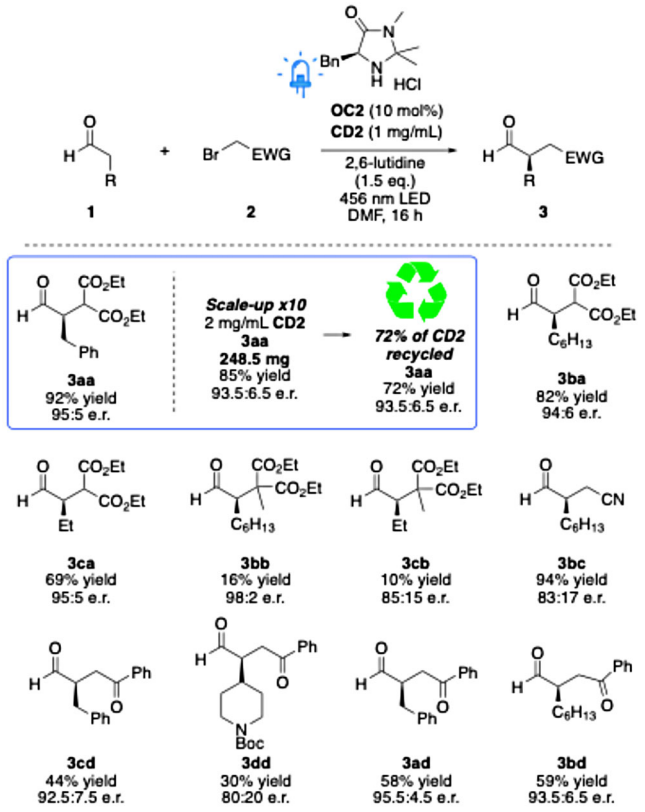

Scheme 2. Substrate scope for the synergistic nano-photo/organocatalytic alkylation of aldehydes. Unless otherwise stated, the reaction conditions were: **1** (0.2 mmol), **2** (0.1 mmol), and DMF (1 mL) at rt for 16 h under inert atmosphere and with degassed solvents. Yield determined via ^{1}H NMR analysis using the internal standard method.

gradually increased from 57 to 73% going from 5 to 1 mg of **CD2**, slightly decreasing to 69% using 0.1 mg of photocatalyst. Nevertheless, even at very low concentrations, the synthesized CDs show a very efficient photocatalytic activity. Furthermore, we also screened different amounts of 2,6-lutidine (Table 2, entries 6–10), observing a decrease of yield below 1 equiv., setting the optimal amount to 1.5 equiv. (Table 2, entry 7).

With the optimized conditions in hand, we explored the scalability of the reaction up to a 1 mmol scale with the model substrates and the recyclability of the catalyst (**Scheme 2**). A 1 mmol-scale reaction yielded the corresponding product **3aa** with comparable excellent yield and enantioselectivity (Scheme 2). In this experiment, we decided to use a 2 mg mL^{-1} solution of CDs, since it gives similar results to the 1 mg mL^{-1}, but it would allow us to try the recycling of the nanocatalysts starting from a higher amount. From this experiment, we were able to successfully isolate 72% of the employed nanophotocatalyst **CD2** by simple water extraction followed by dialysis and subsequent lyophilization of the water phases. The fluorescence and DLS analyses of the used CDs did not show substantial differences with the freshly prepared ones, confirming the high photostability of the designed nanoparticles. Then, the recovered dots were recycled in a subsequent photocatalytic reaction on fresh substrates, which led to the successful production of **3aa** with only a slight erosion of yield and stereoselectivity. This result highlights the potential of carbon nanodots to serve as efficient tools in photocatalytic processes, as heterogeneous recyclable, environmentally friendly and low-cost photosensitizers.

Next, we decided to explore the tolerance of the reaction protocol to structural modifications of the aldehyde and alkylating agent in order to prove the general applicability of the developed methodology. We tested various enolizable aldehydes, paired with bromomalonate **2a**. Comparable good yields and excellent enantioselectivities were obtained by replacing the benzyl substituent with hexyl and ethyl ones (**3ba**, **3ca**), apart from highly sterically hindered aldehydes (see Figure S10, Supporting Information). The reaction proved to be more tolerant to structural alterations on the alkyl bromide. For instance, 2-bromo-2-methylmalonate **2b** afforded the same high level of enantiomeric ratios, albeit at the expense of reactivity in some cases. This could be ascribed to the steric hindrance of the additional methyl that may open competing pathways. Accordingly, in all

© 2025 Wiley-VCH GmbH

16154169, 0, Downloaded from https://advanced.onlinelibrary.wiley.com/doi/10.1002/adsc.202500354 by Fabrizio Vetica - University Di Roma La Sapienza , Wiley Online Library on [16/06/2025]. See the Terms and Conditions (https://onlinelibrary.wiley.com/terms-and-conditions) on Wiley Online Library for rules of use; OA articles are governed by the applicable Creative Commons License

these experiments, the analyses of the nuclear magnetic resonance (NMR) spectra of the crudes evidenced the presence of debrominated methylmalonate, indicating that the photocatalyzed reductive fragmentation took place, but H-atom transfer to the malonate radical competes with the productive addition on the aldehyde. Pleasingly, the reaction could be extended to α-bromo nitriles (**3bc**) and ketones (**3ad**, **3bd**), leading to moderate product formation but excellent enantiomeric ratios, except for product **3ac** (see Figure S10, Supporting Information). Overall, the steric hindrance of both alkylating agent and the substrate is crucial for an efficient reactivity. These results clearly demonstrate the potential of CDs as low-cost and sustainable photocatalysts in asymmetric organophotoredox processes.

Once demonstrated, the general applicability of our procedure, we decided to preliminarily investigate the reaction mechanism. Initially, we decided to perform the experiment in the presence of TEMPO as radical scavenger, which completely prevented product formation, confirming a radical pathway.[16] Then, we wanted to test whether a radical chain path could still promote the formation of the product once the light source was turned off. A light on/off experiment was set up, employing deuterated DMF as solvent in order to monitor the reaction proceeding by NMR analysis (**Figure 2**). It was possible to observe that the light is crucial for the formation of the alkylated product, since no increase of yield was observed after each period of time in the dark. Although light/dark experiments have been widely used to exclude the relevant operation of radical chain pathways, it has been demonstrated that these experiment could not always conclusively exclude radical chains, which could still be possible but impeded by temporal or spatial control, that we took under consideration in our mechanistic proposal (vide infra).[17]

Subsequently, we measured the redox potentials of **CD1** and **CD2** in DMF via cyclic voltammetry (CV) experiments (see Figure S6, Supporting Information). The CVs showed a reduction potential peak at the ground state for **CD2** at –1.86 V and an oxidation peak at +0.90 V versus saturated calomel electrode (SCE). These values are significantly different from those of the prototypical $Ru(bpy)_3$ photocatalyst (Ru^{2+}/Ru^{+} at –1.33 V and Ru^{3+}/Ru^{2+} at +1.29 V) used by MacMillan, which is proposed to operate via a photoreductive pathway (i.e., single eletron tranfer (SET) oxidation of the enamine) in this same transformation. In fact, the oxidation potential for the excited state $*Ru^{2+}/Ru^{3+}$ is −0.81 V, thus being able to reduce diethyl bromomalonate ($E_{red} = -0.62$ V vs. SCE).[18] In contrast, other photosensitizers are proposed to operate via a photo-oxidative pathway, in which the catalysts directly reduce the bromo-derivative to the corresponding alkyl radical and bromide.[5]

For our CDs, the ground state potentials suggest an oxidative quenching pathway due to their easier tendency to be oxidized at the ground state (+0.90 V vs. –1.86 V for the reduction), which is presumably transferred to the excited state. Moreover, fluorescence quenching studies support photo-oxidative quenching. Specifically, fluorescence of **CD2** is not quenched by addition of the aldehyde, **OC2** or both (i.e., the enamine), but only by addition of bromomalonate (**2a**) and 2,6-lutidine (**Figure 3**a; Supporting Information for details).

The crucial presence of 2,6-lutidine for an efficient quenching is still up for debate. It is generally accepted that lutidine only acts as a non-nucleophilic base in these types of photoredox reactions. However, it has been reported by Trapp et al. that 2,6-lutidine is able to form

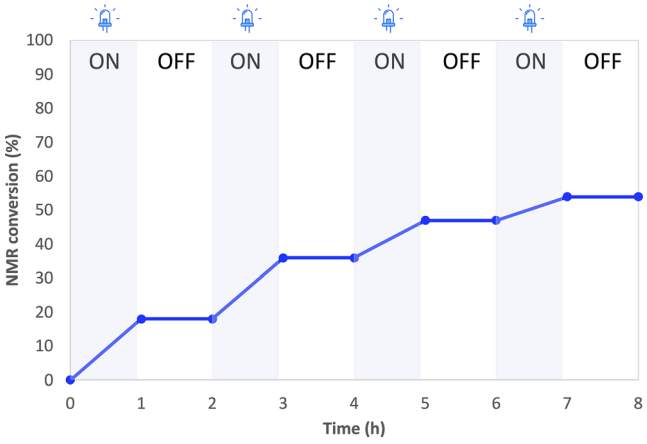

Figure 2. Visible light irradiation on/off experiment for the reaction between **1a** and **2a**, under optimized reaction conditions.

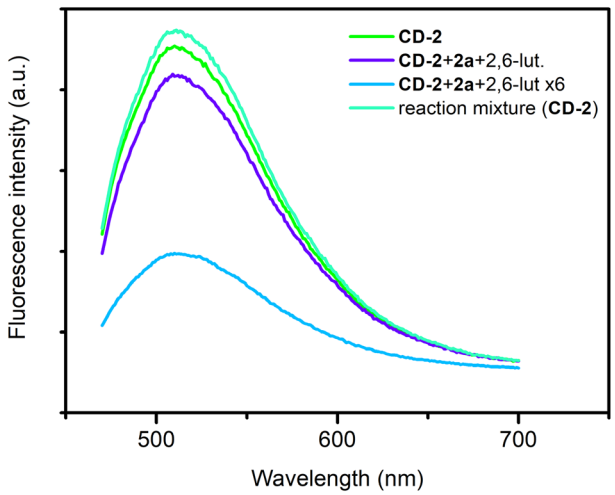

Figure 3. Fluorescence quenching studies of **CD2**. Fluorescence spectra were registered using a 10 μg mL^{-1} solution of **CD2** in DMF, to avoid signal saturation, and keeping the same molecular ratios with the other compounds used in the photochemical reaction: **2a** (2 μmol mL^{-1}), 2,6-lutidine (3 μmol mL^{-1}), **1** (1 μmol mL^{-1}), and **OC2** (0.1 μmol mL^{-1}).

© 2025 Wiley-VCH GmbH

16154169, 0, Downloaded from https://advanced.onlinelibrary.wiley.com/doi/10.1002/adsc.202500354 by Fabrizio Vetica - University Di Roma La Sapienza , Wiley Online Library on [16/06/2025]. See the Terms and Conditions (https://onlinelibrary.wiley.com/terms-and-conditions) on Wiley Online Library for rules of use; OA articles are governed by the applicable Creative Commons License

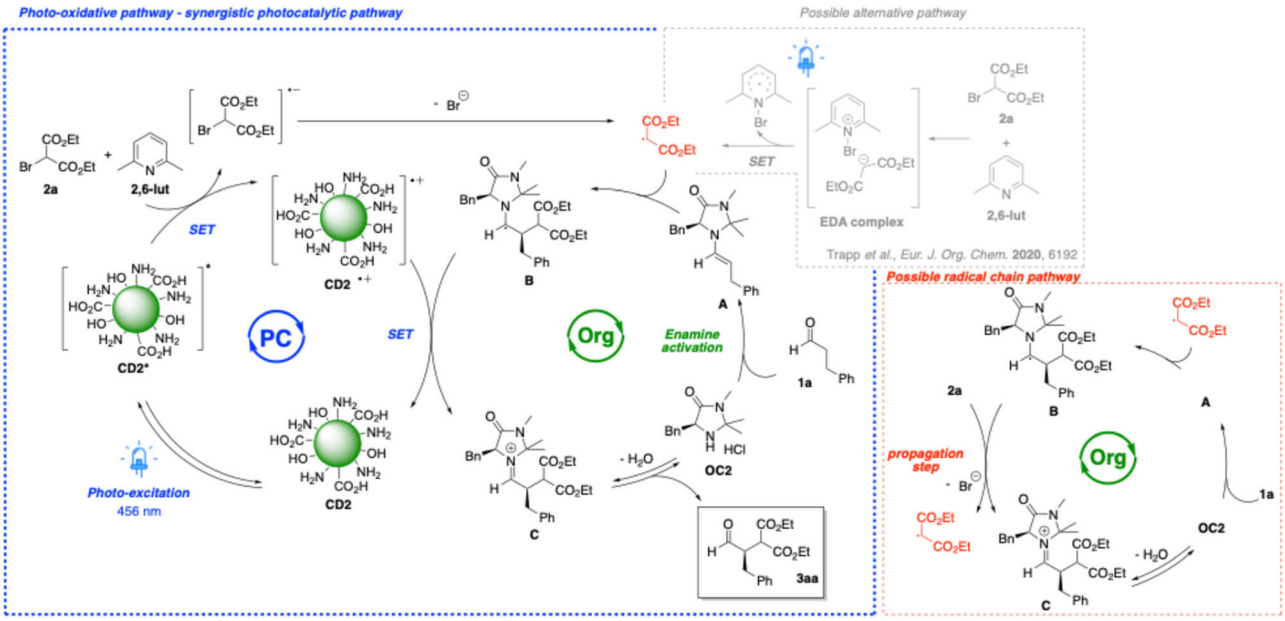

Scheme 3. Postulated reaction mechanism for the synergistic nanophoto/organocatalytic alkylation of aldehydes, involving a photo-oxidative quenching of **CD2** excited state.

an EDA complex with **2a**, which upon blue light irradiation decomposes to lutidine, malonate radical, and bromide anion (see **Scheme 3**) and can thus promote the reaction.[19] The formation of the EDA complex was demonstrated by ultraviolet-visible (UV-vis) spectra, highlighting that the EDA complex is formed after 7 h from mixing the reagents. On the other hand, lutidine can also facilitate reductive quenching of the photocatalyst by deprotonating the radical cation formed upon excitation of the photocatalyst (**CD2**) and its subsequent SET reduction (see Scheme S1, Supporting Information). In fact, the presence of a base in combination with a photocatalyst has been reported to contribute to facilitate oxidation processes.[20] We assumed, on the basis of the above described findings, that we could have the combination of both activities of 2,6-lutidine. In fact, the voltammograms of **CD2** in the presence of lutidine, although do not undergo any shift of the oxidation peaks, show a substantial increase in current intensity, suggesting that the base facilitates the oxidation of **CD2** (see Figure S7, Supporting Information). Moreover, the reaction in the absence of the photocatalyst still proceeds upon irradiation, although with a dramatically lower yield, thus the photoreactivity of the EDA complex is probable. In contrast, when the reaction occurs in the dark, no products at all are observed. We investigated by UV-vis analysis the formation of the EDA complex between **2a** and 2,6-lutidine, observing that no EDA complex was formed right after mixing the reagents, in accordance with Trapp's work (see Figure S8, Supporting Information). While we cannot exclude that overtime some EDA complex can be formed, we proved that at the beginning of the reaction the malonate radical is formed predominantly by the photocatalytic performance of the nanocatalyst. On the basis of our observations and literature precedents, we postulated a possible reaction mechanism, depicted in Scheme 3. A combined photodegradation of the EDA complex and a SET pathway from **CD2***, possibly facilitated by 2,6-lutidine, could concur to generate the bromomalonate radical, which could react with the in situ formed enamine **A**, generated by **OC2** with the aldehyde **1a**. The so-formed iminium radical **B** could be oxidized to the corresponding iminium ion **C** via SET on the **CD2** radical cation, regenerating the ground state of **CD2**. Upon hydrolysis of **C**, the desired enantioenriched alkylated product is afforded, regenerating the organocatalyst **OC2** and thus closing the second catalytic cycle. As previously described, alternative radical propagation steps could not be conclusively excluded. Thus, on the basis of literature reports,[17] we proposed also a possible radical chain alternative pathway, which involve the SET reaction between **B** and **2a** itself, to reform the malonate radical. However, based on our experimental findings, a constant light irradiation is crucial to achieve product formation, predominantly favoring the synergistic catalytic pathway.

3. Conclusion

In conclusion, we reported herein an unprecedented combination of CDs as nanophotocatalyst and stereoselective organocatalysis for the enantioselective α-functionalization of aldehydes, using bromoderivatives as alkylating agents. Various enolizable aldehydes

© 2025 Wiley-VCH GmbH

16154169, 0, Downloaded from https://advanced.onlinelibrary.wiley.com/doi/10.1002/adsc.202500354 by Fabrizio Vetica - University Di Roma La Sapienza , Wiley Online Library on [16/06/2025]. See the Terms and Conditions (https://onlinelibrary.wiley.com/terms-and-conditions) on Wiley Online Library for rules of use; OA articles are governed by the applicable Creative Commons License

and alkylating agents were tested in the optimized conditions, leading to the formation of the desired products with up to 94% yields and up to 98:2 e.r., even at extremely low photocatalyst loadings (down to 0.1 mg mL^{-1}). Furthermore, preliminary mechanistic studies were undertaken to elucidate the reaction pathway of this dual catalytic process and the possibility of recycling the CDs was proved, without hindering the reaction outcomes. The developed protocol could represent an efficient and environmentally friendly tool for synthetic applications, matching the advantages of having nontoxic, biocompatible, and recyclable heterogeneous nanocatalysts with the well-established features of asymmetric organocatalysis in the preparation of optically pure organic compounds.

4. Experimental Section

General Procedure for the Nanophoto/Organocatalytic Alkylation of Aldehydes: **CD2** (1.0 mg) and **OC2** ((*S*)-2-benzyl-3,5,5-trimethylimidazolidin-4-one hydrochloride, 2.55 mg, 0.01 mmol, 10% mol) were added to a 4 mL oven-dried vial equipped with a stirring bar, followed by dimethylformamide (1.0 mL), the aldehyde (0.20 mmol, 2.0 equiv.), the bromide (0.10 mmol, 1.0 equiv.), and 2,6-lutidine (18 µL, 0.15 mmol, 1.5 equiv.). The vial is closed with a rubber cap, and the reaction mixture is degassed by bubbling Ar with a syringe for 20 min. The reaction is set at a distance of 5 cm from a 456 nm Kessil lamp equipped with a cooling fan. After 16 h, the mixture is diluted with brine, extracted with Et_2O (3 × 10 mL), and the reunited organic layers are washed with water (20 mL) and brine (20 mL), dried over anhydrous Na_2SO_4 and reduced in volume through rotary evaporation. The residue is purified with silica gel column chromatography using as eluant mixtures of n-pentane and Et_2O cooled down with liquid N_2 to ensure retention of the enantiomeric ratio before and after the purification of the products. The NMR yields were determined using 1,3,5-trimethoxybenzene (16.82 mg, 0.10 mmol, 1.0 equiv.). For other procedures and literature data, additional references were cited in the Supporting Information.[4,5,7a,14–16,21]

Acknowledgements

Financial support from Sapienza University of Rome (grant number AR1231888BA7F0BA (V.G.M.), RM123188DE5479DA (F.V.), and RM1221814C52ED98 (F.V.)) is gratefully acknowledged. The authors would like to thank Mr. Marco Di Pilato for his help with electrolysis apparatus and Mr. Giulio Papetti for his contribution on initial test trials.

References

[1] a) T. C. Wareing, P. Gentile, A. N. Phan, *ACS Nano* **2021**, *15*, 15471; b) F. Lin, Z. Wang, F.-G. Wu, *Pharmaceuticals* **2022**, *15*, 1236; c) Z.-X. Wang, Z. Wang, F.-G. Wu, *ChemMedChem* **2022**, *17*, e202200003; d) G. Filippini, F. Amato, C. Rosso, G. Ragazzon, A. Vega-Peñaloza, X. Companyó, L. Dell'Amico, M. Bonchio, M. Prato, *Chem* **2020**, *6*, 3022; e) V. Corti, B. Bartolomei, M. Mamone, G. Gentile, M. Prato, G. Filippini, *Eur. J. Org. Chem.* **2022**, *2022*, e202200879; f) G. Gentile, M. Mamone, C. Rosso, F. Amato, C. Lanfrit, G. Filippini, M. Prato, *ChemSusChem* **2023**, *16*, e202202399; g) A. Carioscia, E. Cocco, M. E. Casacchia, G. Gentile, M. Mamone, G. Giorgianni, E. Incerto, M. Prato, F. Pesciaioli, G. Filippini, A. Carlone, *ACS Catal.* **2024**, *14*, 13429; h) X. Pei, D. Xiong, H. Wang, S. Gao, X. Zhang, S. Zhang, J. Wang, *Angew. Chem., Int. Ed.* **2018**, *57*, 3687; i) M. Garrido, L. Gualandi, S. Di Noja, G. Filippini, S. Bosi, M. Prato, *Chem. Commun.* **2020**, *56*, 12698; j) C. Rosso, G. Filippini, M. Prato, *ACS Catal.* **2020**, *10*, 8090; k) C. Rosso, S. Cuadros, G. Barison, P. Costa, M. Kurbasic, M. Bonchio, M. Prato, L. Dell'Amico, G. Filippini, *ACS Catal.* **2022**, *12*, 4290.

[2] a) M. Sbacchi, M. Mamone, L. Morbiato, P. Gobbo, G. Filippini, M. Prato, *ChemCatChem* **2023**, *15*, e202300667; b) Y. Yu, Q. Zeng, S. Tao, C. Xia, C. Liu, P. Liu, B. Yang, *Adv. Mater.* **2023**, *10*, 2207621; c) S. Paul, S. Panja, N. Hazra, K. Gayen, A. Banerjee, *J. Org. Chem.* **2024**, *89*, 91.

[3] a) W. Yao, E. A. Bazan-Bergamino, M.-Y. Ngai, *ChemCatChem* **2022**, *14*, e202101292; b) J.-H. Shen, M. Shi, Y. Wei, *Chem. Eur. J.* **2023**, *29*, e202301157.

[4] D. A. Nicewicz, D. W. C. MacMillan, *Science* **2008**, *322*, 77.

[5] A. Gualandi, M. Marchini, L. Mengozzi, H. T. Kidanu, A. Franc, P. Ceroni, P. G. Cozzi, *Eur. J. Org. Chem.* **2020**, *2020*, 1486.

[6] a) T. He, R. Liu, S. Wang, I. K. W. On, Y. Wu, Y. Xing, W. Yuan, J. Guo, Y. Zhao, *J. Am. Chem. Soc.* **2023**, *145*, 18015; b) T. Rigotti, A. Casado-Sánchez, S. Cabrera, R. Pérez-Ruiz, M. Liras, V. A. de la Peña O'Shea, J. Alemán, *ACS Catal.* **2018**, *8*, 5928.

[7] a) E. Arceo, I. D. Jurberg, A. Álvarez-Fernández, P. Melchiorre, *Nat. Chem.* **2013**, *5*, 750; b) G. E. M. Crisenza, D. Mazzarella, P. Melchiorre, *J. Am. Chem. Soc.* **2020**, *142*, 5461.

[8] Y. Han, H. Huang, H. Zhang, Y. Liu, X. Han, R. Liu, H. Li, Z. Kang, *ACS Catal.* **2014**, *4*, 781.

[9] H. Li, C. Sun, M. Ali, F. Zhou, X. Zhang, D. R. MacFarlane, *Angew. Chem., Int. Ed.* **2015**, *54*, 8420.

[10] a) D. Sarma, B. Majumdar, T. K. Sarma, *Green Chem.* **2019**, *21*, 6717; b) Z. Zhao, B. Pieber, M. Delbianco, *ACS Catal.* **2022**, *12*, 13831; c) B. Bartolomei, V. Corti, M. Prato, *Angew. Chem., Int. Ed.* **2023**, *62*, e202305460; d) K.-K. Niu, C.-Q. Ma, R.-Z. Dong, H. Liu, S.-S. Yu, L.-B. Xing, *Nano Res.* **2024**, *17*, 4825.

[11] M. Mamone, G. Gentile, M. Prato, G. Filippini, *ChemSusChem* **2025**, 2500521.

[12] C. Rosso, G. Filippini, M. Prato, *Chem. Eur. J.* **2019**, *25*, 16032.

[13] a) M. Bortolami, I. I. Bogles, C. Bombelli, F. Pandolfi, M. Feroci, F. Vetica, *Molecules* **2022**, *27*, 5150; b) C. Michenzi, C. Espro, V. Bressi, C. Celesti, F. Vetica, C. Salvitti, I. Chiarotto, *Mol. Catal.* **2023**, *544*, 113182;

 © 2025 Wiley-VCH GmbH

16154169, 0, Downloaded from https://advanced.onlinelibrary.wiley.com/doi/10.1002/adsc.202500354 by Fabrizio Vetica - University Di Roma La Sapienza , Wiley Online Library on [16/06/2025]. See the Terms and Conditions (https://onlinelibrary.wiley.com/terms-and-conditions) on Wiley Online Library for rules of use; OA articles are governed by the applicable Creative Commons License

c) D. Rocco, V. G. Moldoveanu, M. Feroci, M. Bortolami, F. Vetica, *ChemElectroChem* **2023**, *544*, 113182.
[14] E. Sturabotti, A. Camilli, V. G. Moldoveanu, G. Bonincontro, G. Simonetti, A. Valletta, I. Serangeli, E. Miranda, F. Amato, A. G. Marrani, L. M. Migneco, S. Sennato, B. Simonis, F. Vetica, F. Leonelli, *Chem. Eur. J.* **2024**, *30*, e202303631.
[15] A. Di Sabato, F. D'Acunzo, D. Filippini, F. Vetica, A. Brasiello, D. Corinti, E. Bodo, C. Michenzi, E. Panzetta, P. Gentili, *J. Org. Chem.* **2022**, *87*, 13803.
[16] L. Morbiato, L. Cardo, E. Sturabotti, P. Gobbo, G. Filippini, M. Prato, *ACS Nano* **2025**, *19*, 4887.
[17] a) M. A. Cismesia, T. P. Yoon, *Chem. Sci.* **2015**, *6*, 5426; b) B. Reiß, Q. Hu, E. Riedle, H.-A. Wagenknecht, *ChemPhotoChem* **2021**, *5*, 1009.
[18] H. G. Roth, N. A. Romero, D. A. Nicewicz, *Synlett* **2016**, *27*, 714.
[19] E. Fuks, L. Huber, T. Schinkel, O. Trapp, *Eur. J. Org. Chem.* **2020**, *2020*, 6192.
[20] T. Bortolato, G. Simionato, M. Vayer, C. Rosso, L. Paoloni, E. M. Benetti, A. Sartorel, D. Leboeuf, L. Dell'Amico, *J. Am. Chem. Soc.* **2023**, *145*, 1835.
[21] a) E. R. Welin, A. A. Warkentin, J. C. Conrad, D. W. C. MacMillan, *Angew. Chem., Int. Ed.* **2015**, *54*, 9668; b) X. Tian, J. Feng, S. Fan, X. Zhen, J. Han, S. Liu, *Bioorg. Med. Chem.* **2016**, *24*, 5197; c) H.-Y. Jang, J.-B. Hong, D. W. C. MacMillan, *J. Am. Chem. Soc.* **2007**, *129*, 7004; d) M. Silvi, E. Arceo, I. D. Jurberg, C. Cassani, P. Melchiorre, *J. Am. Chem. Soc.* **2015**, *137*, 6120; e) A. Laghezza, C. Cerchia, M. Genovese, R. Leuci, E. Pranzini, A. Santi, L. Brunetti, L. Piemontese, P. Tortorella, A. Biswas, R. P. Singh, S. Tambe, S. Ca, A. K. Pattnaik, V. Jayaprakash, P. Paoli, A. Lavecchia, F. Loiodice, *J. Med. Chem.* **2023**, *66*, 3566; f) T. H. Graham, B. D. Horning, D. W. C. MacMillan, *Org. Synth.* **2011**, *88*, 42; g) L. Dai, Z.-H. Xia, Y.-Y. Gao, Z.-H. Gao, S. Ye, *Angew. Chem., Int. Ed.* **2019**, *58*, 18124.

 © 2025 Wiley-VCH GmbH

16154169, 0, Downloaded from https://advanced.onlinelibrary.wiley.com/doi/10.1002/adsc.202500354 by Fabrizio Vetica - University Di Roma La Sapienza , Wiley Online Library on [16/06/2025]. See the Terms and Conditions (https://onlinelibrary.wiley.com/terms-and-conditions) on Wiley Online Library for rules of use; OA articles are governed by the applicable Creative Commons License